Acta Cryst. (1980). A**36**, 143–146

On the Asymmetric Limits for the Scattering of X-rays from Imperfect Crystals in the Bragg Case

BY S. W. WILKINS

CSIRO Division of Chemical Physics, PO Box 160, *Clayton, Victoria, Australia* 3168

(*Received* 16 *April* 1979; *accepted* 23 *August* 1979)

Abstract

It is pointed out that there is some uncertainty as to the correct behaviour of the integrated reflectivity as a function of the degree of asymmetry for the scattering of X-rays from *imperfect crystals* in the extremely asymmetric Bragg case. Numerical calculations based on the Takagi–Taupin equations are exemplified and indicate that the integrated reflectivity for such crystals tends asymptotically to the perfect-crystal result in the asymmetric limits, the perfect-crystal result, in turn, tends to the kinematical value at these limits, as has been shown previously. In addition, comments are offered on the relevance of the present work to the study of highly imperfect crystals by section topography, and in particular to the study of the near-surface grain-boundary structure of crystals.

Introduction

Recently, Mathieson (1976, 1977) has proposed that the extremely asymmetric Bragg case offers an experimental means for deriving structure factors which is, in principle, free from extinction. The approach is based on the identification of the asymmetric limits ($\beta = \cot\theta_B \tan\alpha \rightarrow \pm 1$, where θ_B is the Bragg angle and α is the asymmetry angle taken as the acute angle between the surface and the Bragg planes, see Fig. 1) as *zero-extinction limits* and requires that data be collected from a given crystal for $|\beta| \rightarrow 1$ and extrapolated to the appropriate limit. The two asymmetric limits are characterized by grazing incidence ($\beta \rightarrow -1$) and grazing emergence ($\beta \rightarrow +1$), see for example Fig. 1 in Wilkins (1978*a*).

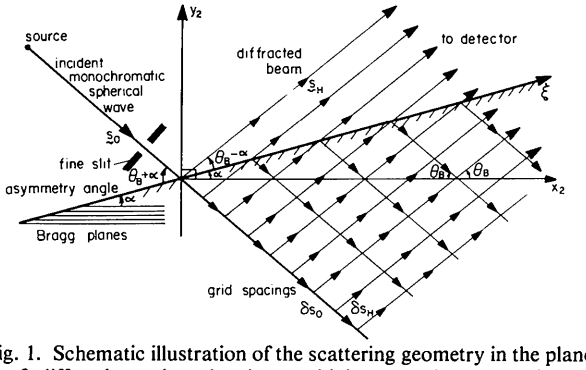

Fig. 1. Schematic illustration of the scattering geometry in the plane of diffraction, also showing multiple scattering paths in the crystal. The vertices of the scattering paths occur as evaluation points in the numerical solution procedure.

Mathieson's method for obtaining extinction-free data depends crucially on the establishment of the asymmetric limits as extinction-free limits. For *perfect crystals*, the validity of this assumption has been demonstrated theoretically by Hirsch & Ramachandran (1950) and by Wilkins (1978*a*). However, for *imperfect crystals*, a reading of the literature would suggest that the situation is not quite so clear.

Thus examination of Darwin's (1922) theoretical expression for secondary extinction in the asymmetric Bragg case (his equation 7.2) shows that $\rho_{\mathrm{Dar}}/\rho_I \nrightarrow 1$ as $\beta \rightarrow \pm 1$, where ρ_{Dar} denotes the integrated reflectivity in Darwin's extinction theory, while ρ_I is the integrated reflectivity for an ideally imperfect crystal (*i.e.* the kinematical approximation value). It should be noted, however, that Darwin's approach is implicitly restricted to small $|\alpha|$ and the concept of correcting integrated reflectivities back to the symmetrical case. More specifically, a key assumption in Darwin's treatment is that the function $G(u)$, giving the scattering per unit path length as a function of rocking angle, u, is independent of α and, in particular, that the contribution of primary extinction (intra-block scattering) to $G(u)$ can be determined in the *symmetrical Bragg case* (Darwin's equations 6.12 to 6.15). This latter assumption would imply, for example, that for $\alpha \neq 0$ one does not regain the perfect-crystal, infinite-thickness result as the block size goes to infinity. Similar assumptions, regarding the form of the scattering per unit path length, to those discussed above are also embodied in the work of Werner (1965) and Werner & Arrott (1965).

Attempts to improve the Darwin treatment by calculating the effect of primary extinction on $G(u)$ in the asymmetric Bragg case are not very satisfactory in the extremely asymmetric regime (Wilkins, 1978*b*; Stephan, 1978) because of the failure of the column approximation.

0567-7394/80/010143-04$01.00

The rigorous treatment of X-ray dynamical scattering from an imperfect crystal is a difficult problem. Kuriyama (1970, 1972) and Kuriyama & Miyakawa (1970) have made valuable contributions to this field *via* a quantum-field-theoretical formulation of the problem. However, the numerical solution of Kuriyama's equations would seem to involve a large amount of computer time compared with the more approximate Takagi–Taupin equations (Takagi, 1962, 1969; Taupin, 1964; Kuriyama, 1972) since his equations involve an extra angular variable describing the spreading out of the diffracted beams due to crystal imperfections. For certain classes of models of an imperfect crystal, and most particularly for a crystal consisting of local mosaic blocks, Kuriyama (1972) has indicated that one can expect the solution of the Takagi–Taupin equations to be very close to the solution of his more accurate equations. In crude terms, one might understand this to be so because the Takagi–Taupin equations are essentially correct for a perfect crystal and so should correctly treat the scattering within perfect-crystal mosaic blocks, while the boundary conditions between blocks may be incorporated *via*, say, an appropriate numerical solution procedure for the equations, as in the present work.

Recently, Kato (1976*a*,*b*) has shown that the Takagi–Taupin equations can be used to provide a unified treatment of primary and secondary extinction. In particular, Kato showed that for different values of the correlation length between lattice distortions, τ, one may obtain the perfect-crystal result (for $\tau \to \infty$), the ideally-imperfect-crystal result (for $\tau \to 0$), and a set of intensity-coupling equations (for τ small).

The work of the above authors suggests that the Takagi–Taupin equations should provide a sound and tractable basis for treating dynamical scattering from a wide class of imperfect crystals, and in particular for investigating the trend in X-ray diffraction properties from imperfect crystals in the approach towards the asymmetric limits. The main purpose of the present note is to present briefly some typical examples of results which have been obtained for the variation of the integrated reflectivity with degree of asymmetry for infinitely thick, imperfect crystals treated in the Bragg case and to present the general conclusions reached on the basis of such calculations. The results were obtained by numerically iterating the Takagi–Taupin equations [equations (11) of Kato (1976*a*)] for given states of the (assumed asymmetric) crystal with simultaneous calculation of the diffracted intensities for various chosen values of the reduced linear absorption coefficient, here defined by

$$\bar{\mu}_0 = \mu_0/|\kappa_{\mathbf{H}}| = -2g_0/(1+\ell^2)^{1/2}, \qquad (1)$$

where μ_0 is the usual linear absorption coefficient, $\ell = \kappa''_{\mathbf{H}}/\kappa'_{\mathbf{H}}$ is the anomalous dispersion parameter ($\kappa'_{\mathbf{H}}$ and $\kappa''_{\mathbf{H}}$ relate to the real and imaginary parts of $\kappa(\mathbf{r})$, respectively), and $1/g_0$ is the level of interaction defined by the second equality in (1) (see also Wilkins, 1978*a*), the superior bar serving here and elsewhere in the text to denote that lengths are measured in reduced units of the inverse coupling coefficient, $1/|\kappa_{\mathbf{H}}|$. The coupling coefficient, $\kappa_{\mathbf{H}}$, for the **H** reflexion with structure factor $F_{\mathbf{H}}$ is given by

$$\kappa_{\mathbf{H}} = \frac{\lambda K}{v}\frac{e^2}{mc^2}F_{\mathbf{H}} \qquad (2)$$

(λ = wavelength, K = polarization factor, v = unit-cell volume and e, m and c are the usual physical constants). A simplifying assumption made throughout the present work is that the refractive index is unity (see also Wilkins, 1978*a*).

General mosaic block model

As a very simple model for treating the displacement parameter, $\mathbf{u}(x_2, y_2)$, in the theory, I have assumed a mosaic block model in which the two-dimensional plane of diffraction is divided into rectangular perfect-crystal blocks of uniform linear dimension, $\bar{l}$, each of which is displaced along the direction of the scattering vector **H** by an amount relative to its neighbours which is sampled from a triangular distribution having standard deviation σ_c. The mosaic blocks are also subject to an angular tilt about their centroids, which is sampled from a triangular distribution having standard deviation σ_b. Configurations of the distorted crystal are generated from strings of random numbers produced by the Fortran subroutine *RANF* on the CSIRO Cyber 76 computer. In mathematical terms, the component of the displacement field **u** along the direction of the scattering vector, **H**, the only component relevant in the present calculations, is given by

$$u_{\parallel}(x_2, y_2) = \sum_{i=1}^{I} c_i^x + \sum_{j=1}^{J} c_j^y + (b_I^x + b_J^y)(\bar{x} - \bar{x}_{IJ}), \quad (3)$$

where I and J are the block-lattice indices along the x_2 and y_2 directions (parallel and perpendicular to Bragg planes, respectively, see also Fig. 1) of the block containing the field point $(\bar{x}_2, \bar{y}_2)$. The coordinate x_2 denotes the distance from the origin along the direction of the Bragg planes, with $\bar{x}_{IJ}$ being the x_2 coordinate of the centroid of the block at block site (I, J). Note that for the sake of brevity the subscript 2 is deleted from coordinates appearing on the right-hand side of (3). The indices i and j run over the block-lattice sites from the origin to (I, J). The block shifts c_i^x and c_j^y are generated from a uniform (square) distribution such that the resulting triangular distribution of $(c_i^x + c_j^y)$ has standard deviation σ_c. The sum of the $(c_i^x + c_j^y)$ produces a random walk, the distribution of the sum tending to normal as the number of steps becomes large. The tilts b_I^x and b_J^y are also sampled from

uniform distributions and the resulting triangular distribution of $(b_j^x + b_j^y)$ has standard deviation σ_b. For the purposes of the present calculation, the parameters σ_b and σ_c are defined such that $u_\parallel$ is measured in units of $1/|\mathbf{H}| = \lambda/\sin\theta_B$.

Results and conclusions

Intensities, $I(\xi)$, on the exit surface for a spherical wave [amplitude $A\delta(s_H)$] incident at $\xi = 0$ on given states of the crystal are plotted in Figs. 2 and 3. For $\beta = 0$ (Fig. 2) and large $\bar{l}$ the curves, such as $\bar{l} = 0{\cdot}5$ and $\bar{l} = 1$, initially follow the perfect-crystal result ($\bar{l} = \infty$), but as ξ/ξ_H becomes larger, detailed structure in the curves appears. For small $\bar{l}$ (say $\bar{l} = 0{\cdot}1$), the curves are highly oscillatory and lie close to the kinematical approximation result ($l \to 0$ and $\sigma_c \neq 0$). In the highly asymmetric regime (Fig. 3), marked changes in the character of the $I(\xi)$ curves are apparent relative to those in Fig. 2. Firstly, most of the fine structure in the curves has disappeared. Secondly, all the curves tend to follow the perfect-crystal result ($\bar{l} = \infty$) rather than the kinematical result. From the results for $I(\xi)$, a corresponding plane-wave-case integrated reflectivity, ρ, was calculated by integrating the individual $I(\xi)$ over the exit surface followed by use of Kato's equation (28*b*). (*N.B.* The present use of this equation implies the simplifying assumption that the *integrated reflectivity* is reasonably independent of the precise entry point of the spherical wave on the crystal surface.) The results for the extinction factor, $y_{\text{ext}} = 1 - \rho/\rho_I$ (where ρ_I is the kinematical approximation value) are plotted in Fig. 4 against the asymmetry parameter $(1 - \beta^2)^{1/2}$ for given values of $\bar{\mu}_0$, $\bar{l}$, σ_b and σ_c. It should be noted that these results were in fact all derived for the positive asymmetry case, but that there exists a statistical form of reciprocity relation between the positive and negative asymmetry cases which shows that the mean (ensemble averaged) value of y_{ext} depends only on $|\beta|$ and not on the sign of β (Wilkins, 1980). From Fig. 4 it can be seen that:

(i) The extinction factor for the perfect-crystal case calculated from the Takagi–Taupin equations agrees well (better than 1%) with the corresponding result (which is accurate to 0·1%) obtained by integrating the plane-wave rocking curves (Wilkins, 1978*a*). This comparison suggests that the accuracy of the numerical solution method for the Takagi–Taupin equations with the chosen grid-size arrangement is probably better than 1% at each β for crystals having *arbitrary* mosaic structure.

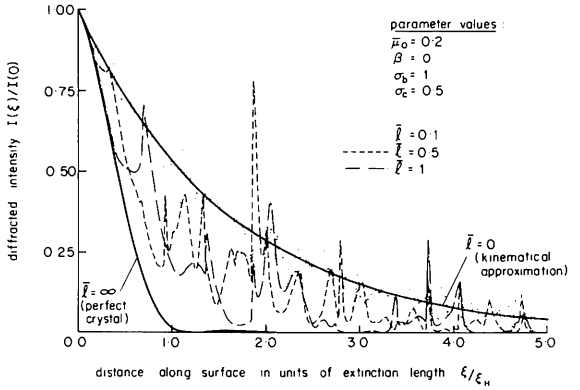

Fig. 2. Intensity profile $I(\xi)/I(0)$ [where $I(0) = A^*A|\kappa_H\kappa_{-H}|\sin^2 2\theta_B$] along the exit surface of the crystal from the entry point measured in units of the extinction length, ξ_H, for a perfect crystal, where $\xi_H = \pi\cos\theta_B/[(1-\beta^2)^{1/2}\cos\alpha|\kappa_H\kappa_{-H}|^{1/2}]$. The results are for the *symmetric Bragg case* ($\beta = 0$) with the following values for the relevant parameters: absorption, $\bar{\mu}_0 = 0{\cdot}2$; Bragg angle, $\theta_B = \pi/9$; block-tilt standard deviation, $\sigma_b = 1$; block-shift standard deviation, $\sigma_c = 0{\cdot}5$; block size, $\bar{l} = 0$, 0·1, 0·5, 1, and ∞. The case $\bar{l} = \infty$ corresponds to the perfect-crystal case, while $\bar{l} = 0$ corresponds to the kinematical approximation.

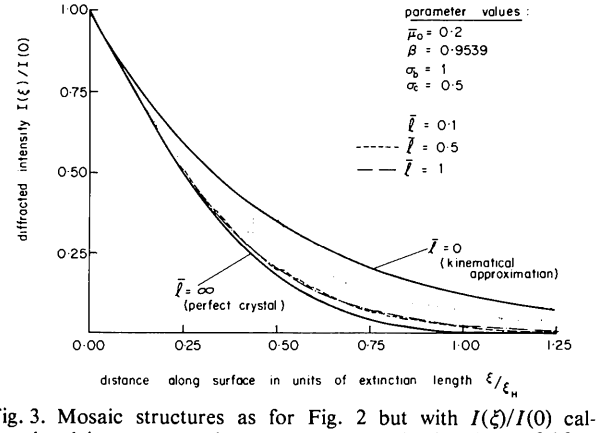

Fig. 3. Mosaic structures as for Fig. 2 but with $I(\xi)/I(0)$ calculated in an extremely *asymmetric case* having $(1-\beta^2)^{1/2} = 0{\cdot}3$; $\beta \simeq 0{\cdot}9539$. The extinction length ξ_H is for a perfect crystal with the given value for β.

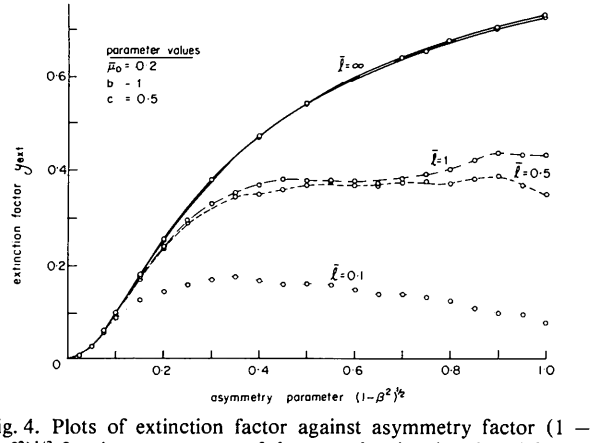

Fig. 4. Plots of extinction factor against asymmetry factor $(1-\beta^2)^{1/2}$ for the *same states of the crystal* as in Figs. 2 and 3. The curves represent guides to the eye through individual data points for a *given state of the crystal*. For $\bar{l} = \infty$, the lower solid curve is the result obtained for a perfect crystal using the present method of numerically solving the Takagi–Taupin equations, while the upper solid curve is that obtained by Wilkins (1978*a*) from numerical integration of the rocking curve.

(ii) The extinction factors plotted in Fig. 4 exhibit somewhat idiosyncratic behaviour because of the sampling of only one member of an ensemble of possible mosaic structures. In practice, for a wide incident beam one should really average $I(\xi)$ over possible entry positions on the crystal surface.

(iii) The extinction factor tends to zero as $|\beta| \rightarrow 1$, thereby supporting Mathieson's postulate.

(iv) The variation in extinction factor with $(1 - \beta^2)^{1/2}$ is no longer necessarily monotonic as it was for infinitely thick, perfect crystals (Wilkins, 1978*a*).

(v) The curves for the imperfect-crystal cases asymptote as $|\beta| \rightarrow 1$ to the corresponding perfect-crystal result (*i.e.* the one having the same absorption coefficient, structure factor, *etc.*).

It should be emphasized at this point that the results presented in Fig. 4 are only *examples* of similar results which have been obtained for a thorough range and combination of parameter values. Thus it appears that the most appropriate mathematical form for the extrapolation of integrated reflectivity data to the asymmetric limits is the perfect-crystal or dynamical-theory result, although the limit itself is the kinematical value. The physical explanation for this behaviour appears to lie in the angular acceptance and divergence characteristics of perfect-crystal scattering volumes as $|\beta| \rightarrow 1$ (see Table 1 in Wilkins, 1978*a*). More particularly, it appears that the *level of interaction* within each block goes to zero as $|\beta| \rightarrow 1$, while the *extent of interaction* (*i.e.* number of blocks which are diffraction coupled) tends to infinity, leading to dominance of dynamical behaviour in the approach to the asymmetric limit due to the latter factor, before final degeneration to kinematical behaviour in the limit due to the former factor (Mathieson, 1979).

It is perhaps interesting to note that results of the type presented in Figs. 2 and 3 suggest that a potentially useful technique for studying the structure and, in particular, the near-surface, grain-boundary structure of a crystal is available by measuring $I(\xi)$. Direct measurement of $I(\xi)$ would, in the language of X-ray topography, correspond to Bragg-case section topographs with an *extremely fine* incident-beam collimator. Slightly less directly, in the case of traverse (projection) topographs, the present work suggests that attainment of optimum resolution of near-surface detail would involve working away from the extremely asymmetric case and using a one-sided slit to eliminate all but the low $|\xi|$ region of $I(\xi)$. Restriction of recorded $I(\xi)$ to low $|\xi|$ would have the added advantage that the data should be interpretable, to a good approximation, using kinematical theory. More generally, one could use a two-sided slit in the diffracted beam to give a projection topograph approximately corresponding to a given depth band in the crystal (see also Lang, 1963).

It also seems worth noting that the present numerical solution scheme offers a very efficient method for calculating section topographs, one line of a section topograph [*i.e.* one $I(\xi)$ curve] taking of the order of 6 s on the CSIRO Cyber 76 computer (see also Petrashen, 1976).

Detailed exploration of the various properties of the general mosaic-block model will be presented elsewhere (Wilkins, 1980).

I am extremely grateful to Dr A. McL. Mathieson for arousing my interest in the present problem and for continued advice and encouragement in its treatment, to Mr A. F. Moodie for helpful discussion, and to Dr S. L. Mair for pointing out that $\rho_{\mathrm{Dar}}/\rho_I \rightarrow 1$.

References

DARWIN, C. G. (1922). *Philos. Mag.* **43**, 800–829.
HIRSCH, P. B. & RAMACHANDRAN, G. N. (1950). *Acta Cryst.* **3**, 187–194.
KATO, N. (1976*a*). *Acta Cryst.* A**32**, 453–457.
KATO, N. (1976*b*). *Acta Cryst.* A**32**, 458–466.
KURIYAMA, M. (1970). *Acta Cryst.* A**26**, 56–59.
KURIYAMA, M. (1972). *Acta Cryst.* A**28**, 588–593.
KURIYAMA, M. & MIYAKAWA, T. (1970). *Acta Cryst.* A**26**, 667–673.
LANG, A. R. (1963). *Br. J. Appl. Phys.* **14**, 904–907.
MATHIESON, A. McL. (1976). *Nature (London)*, **261**, 306–308 [*Erratum: Nature (London)*, **262**, 236].
MATHIESON, A. McL. (1977). *Acta Cryst.* A**33**, 610–617.
MATHIESON, A. McL. (1979). *Acta Cryst.* A**35**, 50–57.
PETRASHEN, P. V. (1976). *Sov. Phys. Solid State*, **18**, 2175–2176.
STEPHAN, D. (1978). *Krist. Tech.* **13**, 155–163.
TAKAGI, S. (1962). *Acta Cryst.* **15**, 1311–1312.
TAKAGI, S. (1969). *J. Phys. Soc. Jpn*, **26**, 1239–1253.
TAUPIN, D. (1964). *Bull. Soc. Fr. Minéral. Cristallogr.* **87**, 469–511.
WERNER, S. (1965). PhD thesis. Univ. of Michigan.
WERNER, S. & ARROT, A. (1965). *Phys. Rev.* **140**, 675–686.
WILKINS, S. W. (1978*a*). *Proc. R. Soc. London Ser. A*, **364**, 569–589.
WILKINS, S. W. (1978*b*). Unpublished.
WILKINS, S. W. 1980). In preparation.